

Dynamic Dyadic Green Function Formalism for Uniaxial Metamaterials

Hodjat Mariji *

Stanislav I. Maslovski †

Departamento de Engenharia Electrotécnica, Instituto de Telecomunicações, Universidade de Coimbra, Pólo II, 3030-290 Coimbra, Portugal

Abstract

Based on the dynamic dyadic Green's function (DDGF) method, we present a self-consistent formalism to study the propagation of electromagnetic fields with slowly varying amplitude (EMFSVA) in a dispersive anisotropic metamaterial with two dyadic constitutive parameters, the dielectric permittivity and the magnetic permeability. We find the matrix elements of DDGFs by applying the formalism for uniaxial anisotropic metamaterials. We present the relations for the velocity of narrow-band EMFSVA envelops which agree with the known definition of the group velocity in dispersive media. We consider the examples of superluminal and subluminal propagation of EMFSVA passing through active and passive non-magnetic media with Lorentz and Drude type dispersions. Considering a source in the form of a Gaussian pulse and defining equivalent Huygens surface currents on the interfaces of a three-layer impedance matched slab with an active substance in the middle, we simulate the propagation of the EMFSVA pulses. The results of this paper are applicable to the propagation of electromagnetic fluctuations through dispersive anisotropic media and microwave devices such as waveguides and delay lines.

1 Introduction

Nowadays, there has been a growing interest in metamaterials (MMs) which are artificial composites used in various branches of science and engineering. After the pioneering works on the backward waves propagation in media [1]–[4], many scientists have focused on the appealing feature — negative refractive index, of active and passive MMs [5, 6], and on the applications of MMs for modeling of general relativity effects with artificial black holes [7], for remarkable control over electromagnetic fields [8], novel optical phenomena such as perfect electromagnetic absorber [9, 10], diffraction-unlimited imaging [11], invisible cloaking [12], as well as to designing MMs for special goals, for instance, to achieve frequency-agile or multi-band operating [13]–[15], to mediate repulsive Casimir force [16], to access low-loss in optical frequency [17], to tune microwave light [18], and to fabricate flat lenses [19]. One of the broad impacts of MMs which has attracted science and technology attention concerns with the study on the near field radiative heat transfer and super-Planckian thermonics [20]–[22] with applications for thermophovoltaic technology [23, 24].

The unusual dispersive properties of the MM result, in some situations, in superluminal or subluminal group velocities $V_g = \partial\omega/\partial k$, in which case this quantity can be higher or extremely lower than the light speed in vacuum. It can even become zero or negative [25]–[28]. It is worth to mention that this superluminal effect, as well as the negative refraction index, are well-accommodated within the framework of the causality principle [29]–[32]. In recent decades, superluminal and subluminal group velocities have attracted attentions in nonlinear optics [33], quantum communication [34], photon controlling and storage [35]–[37], precision sensing [38], high-speed optical switching [39, 40], broadband electromagnetic devices, and delay compensation circuits in ultra-high-speed communication systems [41], in addition to compact high resolution spectrometers [42].

In this article, based on the dynamic dyadic Green's function (DDGF) method, we present a self-consistent formalism to solve the Maxwell equations for the electromagnetic fields with slowly varying amplitude (EMFSVA) which propagate through a dispersive anisotropic medium with known permittivity and permeability dyadics. This formalism can be employed for any type of local media with frequency dispersion, for example, to study the propagation of electromagnetic field fluctuations, such as in the near-field radiative heat transfer, which is one of the actively developing topics in MM applications context. In the current work, we examine our formalism on non-magnetic uniaxial MMs and media with gain to study the superluminal and subluminal behavior of the group velocity in passive and active materials. It is worth to mention that uniaxial anisotropic MMs are simpler to realize and due to that they attract more interest. In addition, they are known for advantageous optical properties for sensing [43], nonlinear optical applications [44], and spontaneous emission control [45].

We introduce the group velocity of EMFSVA for the transverse electric and magnetic polarizations (TE and TM), by extracting poles of the Fourier-transformed Green function in the complex plane of the axial wave number. In order to study the superluminal propagation of EMFSVA, we apply our formalism for a three-layer slab in which an active medium, e.g. inverted population ^{132}Xe gas, has been sandwiched between two passive dielectric layers. We consider that when a primary pulse excited by a Gaussian source passes through the passive layer, the transverse

*E-mail: hodjat.mariji@uc.pt, astrohodjat@gmail.com

†E-mail: stas@co.it.pt

electric and magnetic fields at the interface of the next layer can be regarded as equivalent Huygens sources [46] (pairs of electric and magnetic surface currents), which act as secondary excitations for the next layers. The layers are assumed non-magnetic and impedance-matched so that there are no reflections at the interfaces. In practice, approximate impedance matching is achieved when the permittivities of the passive layers are the same as the real part of the permittivity of the active layer.

This paper is organized as follows: in Sec. 2, we briefly set up the main tools to be used in our formalism for the EMFSVA; in Sec. 3, which employs the DDGF technique, the formalism is presented; in Sec. 4, we obtain the DDGF matrix elements for the uniaxial anisotropic MMs; in Sec. 5, we study superluminal and subluminal group velocities of EMFSVA in active and passive media. Finally, we shall discuss results and draw conclusions in Sec. 6.

2 Main EMFSVAs Tools and Definitions

In order to investigate the propagation of EMFSVA in a dispersive medium, we consider the Maxwell equations for the time-dependent electromagnetic fields and sources written as follows:

$$\nabla \cdot \vec{D} = \rho^E, \quad \nabla \cdot \vec{B} = \rho^M, \quad \nabla \times \vec{E} = -\partial_t \vec{B} - \vec{J}^M, \quad \nabla \times \vec{H} = \partial_t \vec{D} + \vec{J}^E, \quad (1)$$

where the vectors \vec{E} , \vec{H} , \vec{D} , and \vec{B} are the electric field, the magnetic field, the electric displacement, and the magnetic flux density, respectively, and $\partial_t = \frac{\partial}{\partial t}$. In Eq. (1), $\rho^{E(M)}$ and $\vec{J}^{E(M)}$, the electric (magnetic) charge and current densities, respectively, are related by the continuity equation, $\nabla \cdot \vec{J}^{E(M)} + \partial_t \rho^{E(M)} = 0$. The electromagnetic constitutive equation is given by

$$\vec{\Xi} = \bar{\bar{\zeta}} \cdot \vec{F}, \quad (2)$$

where the dyadic operator $\bar{\bar{\zeta}} = \bar{\bar{\varepsilon}} (\bar{\bar{\mu}})$ formally represents the dispersive permittivity (permeability) tensor of the material, which relates $\vec{\Xi} = \vec{D}(\vec{B})$ to $\vec{F} = \vec{E}(\vec{H})$.

The time-dependent electromagnetic field can be expanded into the monochromatic spectral components as follows

$$\vec{F}(t) = \frac{1}{2\pi} \int_{-\infty}^{+\infty} \vec{F}(\omega) e^{-i\omega t} d\omega. \quad (3)$$

On the other hand, considering the time-harmonic fields with slowly varying amplitude (SVA), it is acceptable that the most spectral energy is concentrated in a narrow band $\Delta\omega$ around ω_0 , the carrier frequency, with $\Delta\omega \ll \omega_0$. Thus, we can define the EMFSVA, $\vec{F}_m(t)$, as follows

$$\vec{F}(t) = \frac{1}{2} \vec{F}_m(t) e^{-i\omega_0 t} + c.c., \quad \vec{F}_m(t) = \frac{1}{\pi} \int_{-\Delta\omega/2}^{+\Delta\omega/2} \vec{F}(\omega_0 + \Omega) e^{-i\Omega t} d\Omega, \quad (4)$$

where *c.c* is the abbreviation for the complex conjugate of the previous term and $\Omega = \omega - \omega_0$. We also assume that $\bar{\bar{\zeta}}$ has appreciably smooth behavior in the narrow band $\Delta\omega$, which is a reasonable assumption for applications of our interest. So, expanding $\bar{\bar{\zeta}}$ around ω_0 and keeping only two first terms, we obtain

$$\bar{\bar{\zeta}}(\omega) = \bar{\bar{\zeta}}_{\omega_0} + (\partial_\omega \bar{\bar{\zeta}})_{\omega_0} \Omega, \quad (5)$$

where the subscript ω_0 denotes the quantity which is computed at ω_0 and $\partial_\omega = \frac{\partial}{\partial \omega}$. Using Eq. (5) and ignoring the second and higher orders of the time-derivative of \vec{F}_m , we obtain $\partial_t \vec{\Xi}$ as follows

$$\partial_t \vec{\Xi} = [\partial_t \vec{\Xi}_m(t) - i\omega_0 \vec{\Xi}_m(t)] e^{-i\omega_0 t}, \quad \vec{\Xi}_m(t) = \bar{\bar{\zeta}}_{\omega_0} \cdot \vec{F}_m + (\partial_\omega \bar{\bar{\zeta}})_{\omega_0} \cdot \partial_t \vec{F}_m. \quad (6)$$

With having these tools at hand, we proceed to the Green's Function technique to solve the Maxwell equations and to obtain \vec{F}_m in the next section.

3 DDGF Technique

Starting from the third and forth equations of Eq. (1) for the time-harmonic complex electromagnetic fields and sources and using Eq. (2) and the subsequent equations, the Maxwell 6-vector equations assume the following operator form:

$$\hat{\mathbf{O}} \cdot \vec{F}_m = -i \vec{J}_m. \quad (7)$$

In the above equation, \vec{F}_m , the 6-vector field, $\hat{\mathbf{O}}$, the electromagnetic operator, and \vec{J}_m , the 6-vector current, are given by

$$\vec{F}_m \doteq \begin{bmatrix} \vec{E}_m \\ \vec{H}_m \end{bmatrix}, \quad \hat{\mathbf{O}} \doteq i \begin{bmatrix} (\partial_t - i\omega_0) \bar{\bar{\varepsilon}} & -\nabla \times \bar{\bar{I}} \\ \nabla \times \bar{\bar{I}} & (\partial_t - i\omega_0) \bar{\bar{\mu}} \end{bmatrix}, \quad \vec{J}_m \doteq \begin{bmatrix} \vec{J}_m^E \\ \vec{J}_m^M \end{bmatrix}, \quad (8)$$

where $\bar{\bar{I}}$ is the unity dyadic. Replacing the distributed electric and magnetic current sources by the point ones, we introduce the dynamic dyadic Green's Function (DDGF), such that

$$\hat{\mathbf{O}} \cdot \bar{\bar{\mathbf{G}}} = -i\bar{\bar{I}}. \quad (9)$$

The above means that the elements of DDGF are obtained by constructing \mathbf{O}^{-1} , the matrix of the operator inverse to $\hat{\mathbf{O}}$, that is, $(\bar{\bar{\mathbf{G}}})_{pq} = -i(\mathbf{O}^{-1})_{pq}$. Thus, Eq. (8) can be expanded as follow

$$(\partial_t - i\omega_0)\bar{\varepsilon} \cdot \bar{\bar{\mathbf{G}}}_{11} - \nabla \times \bar{\bar{I}} \cdot \bar{\bar{\mathbf{G}}}_{21} = -\bar{\bar{I}}, \quad (\partial_t - i\omega_0)\bar{\varepsilon} \cdot \bar{\bar{\mathbf{G}}}_{12} - \nabla \times \bar{\bar{I}} \cdot \bar{\bar{\mathbf{G}}}_{22} = \bar{\bar{0}}, \quad (10)$$

$$(\partial_t - i\omega_0)\bar{\mu} \cdot \bar{\bar{\mathbf{G}}}_{21} + \nabla \times \bar{\bar{I}} \cdot \bar{\bar{\mathbf{G}}}_{11} = \bar{\bar{0}}, \quad (\partial_t - i\omega_0)\bar{\mu} \cdot \bar{\bar{\mathbf{G}}}_{22} + \nabla \times \bar{\bar{I}} \cdot \bar{\bar{\mathbf{G}}}_{12} = -\bar{\bar{I}}, \quad (11)$$

where $\bar{\bar{0}}$ is the null dyadic.

It is more convenient to work in the Fourier space. We define $\bar{\bar{\mathbf{g}}}$, the Fourier transform of DDGF, as

$$\bar{\bar{\mathbf{G}}}(\vec{R}, \tau) = \frac{1}{(2\pi)^4} \int d\vec{k} \int_{-\Delta\omega/2}^{+\Delta\omega/2} d\Omega \bar{\bar{\mathbf{g}}}(\vec{k}, \Omega) e^{i(\vec{k} \cdot \vec{R} - \Omega\tau)}, \quad \vec{R} = \vec{r} - \vec{r}', \quad \tau = t - t'. \quad (12)$$

Recalling Eq. (7) and using that, in the Fourier space, $\partial_t = -i\Omega$ and $\nabla = i\vec{k}$, where \vec{k} is wave vector, the 6-vector equation gets

$$\hat{\mathbf{O}} \cdot \bar{\bar{\mathbf{F}}}_m = -i\bar{\bar{\mathbf{J}}}_m, \quad \hat{\mathbf{O}} \doteq \begin{bmatrix} D_\Omega \bar{\bar{\zeta}}_\Omega & \vec{k} \times \bar{\bar{I}} \\ -\vec{k} \times \bar{\bar{I}} & D_\Omega \bar{\bar{\mu}}_\Omega \end{bmatrix}, \quad (13)$$

where the differential operator D_Ω is defined by $D_\Omega \bar{\bar{\zeta}}_\Omega = \omega_0 \bar{\bar{\zeta}}_{\omega_0} + \Omega \left[\partial_\omega (\omega \bar{\bar{\zeta}}_\Omega) \right]_{\omega_0}$ and $\bar{\bar{\zeta}}_\Omega$ is the Fourier transform of $\bar{\bar{\zeta}}$. Now, Eqs. (9) gets following forms:

$$\hat{\mathbf{O}} \cdot \bar{\bar{\mathbf{g}}} = -i\bar{\bar{I}}, \quad (14)$$

Knowing the tensor form of the constitutive parameters of the medium and solving the above equations, we can obtain $\bar{\bar{\mathbf{g}}}$ and, in turn, DDGF. Afterward, for any given forms of the electric and magnetic source functions, the components of 6-vector $\bar{\bar{\mathbf{F}}}_m$ are obtained by the operator equation or by the integral one as follows

$$\bar{\bar{\mathbf{F}}}_m = \bar{\bar{\mathbf{G}}} \cdot \bar{\bar{\mathbf{J}}}_m, \quad \text{or} \quad \bar{\bar{\mathbf{F}}}_m(\vec{r}, t) = \int \bar{\bar{\mathbf{G}}}(\vec{r} - \vec{r}'; t - t') \cdot \bar{\bar{\mathbf{J}}}_m(\vec{r}', t') d^3r' dt'. \quad (15)$$

In the next subsection, we shall find the matrix elements of DDGF for uniaxial anisotropic media.

4 DDGFs Matrix Elements

We apply the DDGF technique for uniaxial anisotropic media to obtain the matrix elements. For uniaxial media we can write

$$\bar{\bar{\zeta}} = \zeta_t \bar{\bar{I}}_t + \zeta_z \bar{\bar{I}}_z \quad (16)$$

with $\bar{\bar{I}}_t = \hat{x}\hat{x} + \hat{y}\hat{y}$ and $\bar{\bar{I}}_z = \hat{z}\hat{z}$ as the identity dyadics in two orthogonal directions, that is, the tangential and axial (the main axis) directions, respectively, along which the electromagnetic responses of the medium are not the same. In order to obtain the DDGF of the uniaxial medium, we impose this property of constitutive parameters to decompose Eq. (13) as

$$\hat{\mathbf{O}} \doteq \begin{bmatrix} D_\Omega \varepsilon_t \bar{\bar{I}}_t & \bar{\bar{0}} & \vec{k}_z \times \bar{\bar{I}}_t & \vec{k}_t \times \bar{\bar{I}}_z \\ \bar{\bar{0}} & D_\Omega \varepsilon_z \bar{\bar{I}}_z & \vec{k}_t \times \bar{\bar{I}}_t & \bar{\bar{0}} \\ -\vec{k}_z \times \bar{\bar{I}}_t & -\vec{k}_t \times \bar{\bar{I}}_z & D_\Omega \mu_t \bar{\bar{I}}_t & \bar{\bar{0}} \\ -\vec{k}_t \times \bar{\bar{I}}_t & \bar{\bar{0}} & \bar{\bar{0}} & D_\Omega \mu_z \bar{\bar{I}}_z \end{bmatrix}, \quad (17)$$

where we dropped the dependency on Ω from $\bar{\bar{\zeta}}_{t(z)}$ and $\bar{\bar{\mu}}_{t(z)}$. When writing the matrix elements in Eq. (17), we keep in mind that $\vec{k} \times \bar{\bar{I}} = (\vec{k}_t + \vec{k}_z) \times (\bar{\bar{I}}_t + \bar{\bar{I}}_z)$. It is more convenient if we replace the second row with the third one and also the third column with the second one of the block matrix representation of $\hat{\mathbf{O}}$ so that the tangential and axial components of the constitutive parameters of the medium take place in the separate blocks and, in turn, it is also necessary that we rearrange the tangential and z components of $\bar{\bar{\mathbf{F}}}_m$ together with those of $\bar{\bar{\mathbf{J}}}_m$. Now, regarding Eq. (14), DDGF is obtained by computing the inverse of \mathbf{O} as

$$\begin{bmatrix} \bar{\bar{\mathbf{g}}}_{EE} & \bar{\bar{\mathbf{g}}}_{EM} \\ \bar{\bar{\mathbf{g}}}_{ME} & \bar{\bar{\mathbf{g}}}_{MM} \end{bmatrix} = -i \begin{bmatrix} \bar{\bar{\mathbf{O}}}_{11} & \bar{\bar{\mathbf{O}}}_{12} \\ \bar{\bar{\mathbf{O}}}_{21} & \bar{\bar{\mathbf{O}}}_{22} \end{bmatrix}^{-1} \cdot \begin{bmatrix} \bar{\bar{I}}_{tt} & \bar{\bar{0}} \\ \bar{\bar{0}} & \bar{\bar{I}}_{zz} \end{bmatrix}, \quad (18)$$

where $\bar{\bar{I}}_{tt}$ and $\bar{\bar{I}}_{zz}$ are given by

$$\bar{\bar{I}}_{tt} \doteq \begin{bmatrix} \bar{\bar{I}}_t & \bar{\bar{0}} \\ \bar{\bar{0}} & \bar{\bar{I}}_t \end{bmatrix}, \quad \bar{\bar{I}}_{zz} \doteq \begin{bmatrix} \bar{\bar{I}}_z & \bar{\bar{0}} \\ \bar{\bar{0}} & \bar{\bar{I}}_z \end{bmatrix}. \quad (19)$$

In Eq. (18), $\bar{\bar{g}}_{EE}$ ($\bar{\bar{\mathbf{O}}}_{11}$), $\bar{\bar{g}}_{EM}$ ($\bar{\bar{\mathbf{O}}}_{12}$), $\bar{\bar{g}}_{ME}$ ($\bar{\bar{\mathbf{O}}}_{21}$), and $\bar{\bar{g}}_{MM}$ ($\bar{\bar{\mathbf{O}}}_{22}$), are 4×4 , 4×2 , 2×4 , and 2×2 matrices in which we have used the customary notation for the indices of the $\bar{\bar{g}}$ elements. Decomposing the fields into two orthogonal polarizations, TE and TM, and introducing new notations for the TM and TE polarizations as follows

$$D_\Omega \varepsilon_i = \kappa_i, \quad \kappa_i = a_i + b_i \Omega, \quad a_i = (\omega \varepsilon_i)_{\omega_0}, \quad b_i = [\partial_\omega (\omega \varepsilon_i)]_{\omega_0}, \quad (\text{TM}) \quad (20)$$

$$D_\Omega \mu_i = \kappa_i^*, \quad \kappa_i^* = a_i^* + b_i^* \Omega, \quad a_i^* = (\omega \mu_i)_{\omega_0}, \quad b_i^* = [\partial_\omega (\omega \mu_i)]_{\omega_0}, \quad (\text{TE}) \quad (21)$$

where the index i denotes t and z . So, all quantities with *star* (*) belong to the TE polarization. Now, using Eqs. (18)-(21), and employing vector and dyadic algebras together with some manipulations, we obtain 18 non-zero matrix elements of $\bar{\bar{g}}$ as follows

$$g_{EE}^{11[33]} = i \frac{\kappa_t^* [\kappa_t] - \kappa_z^{*-1} k_t^2}{\kappa^{*2} - k_z^2}, \quad g_{EE}^{14} = g_{EE}^{41} = i \frac{k_z}{\kappa^2 - k_z^2}, \quad g_{EE}^{23} = g_{EE}^{32} = i \frac{-k_z}{\kappa^{*2} - k_z^2}, \quad g_{EE}^{44[22]} = i \frac{\kappa_t^*}{\kappa^{*2} - k_z^2}, \quad (22)$$

$$g_{MM}^{11[22]} = -i \frac{\kappa_z^{*-1} (\kappa_t \kappa_t^* - k_z^2)}{\kappa^{*2} - k_z^2}, \quad g_{EM}^{11[23]} = i \frac{-\kappa_z^{*-1} k_t k_z}{\kappa^{*2} - k_z^2}, \quad g_{EM}^{41[22]} = i \frac{\kappa_t^* \kappa_z^{*-1} k_t}{\kappa^{*2} - k_z^2}, \quad g_{ME}^{mn} = -g_{EM}^{nm}, \quad (23)$$

where κ^{*} are given by

$$\kappa^{*2} = \kappa_t \kappa_t^* - \kappa_t^* \kappa_z^{*-1} k_t^2, \quad (24)$$

In the above equations, we use shortened forms like $A^{ij[kl]} = f^{*}[h]$ which means $A^{ij} = f$ and $A^{kl} = f^* h$. We keep this type of shortened form in the rest of this paper. As can be seen in the above equations, there are two poles $\pm \kappa$ for the TM-polarized propagation and, similarly, $\pm \kappa^*$ for the TE one, where \pm are related to the upper/lower half-plane of k_z complex plane for $Z \gtrless 0$ propagation. Recalling Eq. (15) and breaking down $\vec{k} \cdot (\vec{r} - \vec{r}')$ as $\vec{k}_t \cdot \vec{\varrho} + \vec{k}_z \cdot \vec{Z}$ with $\vec{\varrho} = (\vec{\rho} - \vec{\rho}')$ and $\vec{Z} = (z - z')\hat{z}$, we can integrate over k_z in the complex plane. There are two categories of answers, with respect to denominators of $\bar{\bar{g}}$ matrix elements (cf. Eqs. (22)-(23)), as follows

$$g_{\alpha\beta}^{mn}(\vec{k}_t, \pm \kappa^{*}, \Omega; \pm |Z|) = N_{\alpha\beta}^{mn}(\vec{k}_t, \pm \kappa^{*}, \Omega) e^{i\kappa^{*}|Z| - \Omega\tau} \begin{Bmatrix} 1/\kappa^{*} \\ 1 \end{Bmatrix}, \quad (25)$$

where $N_{\alpha\beta}^{mn}$ are the corresponding terms of numerators in $g_{\alpha\beta}^{mn}$ with $m, n = 1, \dots, 4$ and $\alpha, \beta = E, M$.

Remembering EMFSVAs, we expand κ^{*} around $\Omega = 0$ and ignore $O(\Omega^2)$ terms so that

$$\kappa^{*} = \kappa_{\Omega=0}^{*} + \Omega \left(\frac{\partial \kappa^{*}}{\partial \Omega} \right)_{\Omega=0}. \quad (26)$$

We define the group velocity, v_g^{*} , of EMFSVAs by

$$V_g^{*} = \text{Re}(V_g^{*}), \quad V_g^{*} = \left(\frac{\partial \kappa^{*}}{\partial \Omega} \right)_{\Omega=0}^{-1} \quad (27)$$

and obtain

$$V_g^{*} = \frac{2\kappa_0^{*}}{(a_t b_t^* + a_t^* b_t) - (b_t^{*2} a_z^{*2} - a_t^{*2} b_z^{*2}) k_t^2 / a_z^{*2}}, \quad \kappa_0^{*} = \sqrt{a_t a_t^* - \frac{a_t^{*2}}{a_z^{*2}} k_t^2}, \quad (28)$$

for the TM [TE] polarization. In Sec. III, we present a closer look on the group velocity for a propagating envelop within active and passive dispersive anisotropic media. We shall show that ignoring the second order term in Eq. (26) is reasonable for most of the interesting frequency intervals.

Now, we have three categories of integrals over Ω for different matrix elements of DDGF, as follows

$$e^{i\kappa_0^{*} Z} \int_{-\Delta\omega/2}^{+\Delta\omega/2} d\Omega e^{i\tau_g^{*} \Omega} \begin{Bmatrix} 1 \\ \frac{1}{\kappa_z^{*}(\Omega)} \\ \frac{f^{*}(\Omega)}{\kappa^{*}(\Omega)} \end{Bmatrix}, \quad \tau_g^{*} = Z/V_g^{*} - \tau^{*}, \quad (29)$$

where $f^{*}(\Omega)$ are the corresponding functions in the numerators of $\bar{\bar{g}}$ matrix elements (cf. Eqs. (22)-(23)). The first integral category leads to the zeroth order of the spherical Bessel function, j_0 . Recalling Taylor's expansion for $1/\kappa_z^{*}$ around $\Omega = 0$, by ignoring $O(\Omega^2)$, the second and third integral categories in Eq. (29) lead to a linear combination of j_0 and j_1 , the first order of the spherical Bessel function. So, the matrix elements of $\bar{\bar{\mathbf{G}}}(k_t, \vec{\varrho}, Z; \Delta\omega, \tau)$ are given by

$$\bar{\bar{\mathbf{G}}} = \frac{1}{(2\pi)^3} e^{i\kappa_0^{*}|Z|} \int d\vec{k}_t e^{i\vec{k}_t \cdot (\vec{\varrho} - \vec{\varrho}')} \left(\frac{\Delta\omega}{2} \right) \left\{ \bar{\bar{\mathbf{C}}} \left[j_0(\tau_g^{*} \Delta\omega/2) \right] - i \bar{\bar{\mathbf{D}}} \left[\left(\frac{\Delta\omega}{2} \right) j_1(\tau_g^{*} \Delta\omega/2) \right] \right\} \quad (30)$$

where $\overline{\overline{\mathbf{C}}}$ and $\overline{\overline{\mathbf{D}}}$ are given by:

$$\overline{\overline{\mathbf{C}}} \doteq \begin{bmatrix} C_{EE} & C_{EM} \\ C_{ME} & C_{MM} \end{bmatrix}, \quad \overline{\overline{\mathbf{D}}} \doteq \begin{bmatrix} D_{EE} & D_{EM} \\ D_{ME} & D_{MM} \end{bmatrix}. \quad (31)$$

The non-zero elements of $C_{\alpha\beta}$ and $D_{\alpha\beta}$ matrices are as follows

$$C_{EE}^{11[33]} = \frac{a_z a_t^* [a_z^* a_t] - k_t^2}{a_z^{[\star]} \kappa_0^{[\star]}}, \quad C_{EE}^{44[22]} = \frac{a_t^{[\star]}}{\kappa_0^{[\star]}}, \quad C_{EE}^{14} = C_{EE}^{41} = -C_{EE}^{23} = -C_{EE}^{32} = n_z, \quad (32)$$

$$D_{EE}^{11[33]} = \frac{(a_z a_t^* [a_z^* a_t] - k_t^2) (a_z^{[\star]} V_g^{[\star]-1} + b_z^{[\star]} \kappa_0^{[\star]}) - (a_z a_t^* [a_z^* b_t] + b_z a_t^* [b_z^* a_t])}{a_z^{[\star]} \kappa_0^{[\star]}}, \quad D_{EE}^{44[22]} = \frac{a_t^{[\star]} V_g^{[\star]-1} - b_t^{[\star]} \kappa_0^{[\star]}}{\kappa_0^{[\star]2}}, \quad (33)$$

$$C_{MM}^{11[22]} = \frac{a_t^{[\star]} k_t^2}{\kappa_0^{[\star]} a_z^{[\star]2}}, \quad D_{MM}^{11[22]} = \left(\frac{a_t^{[\star]} V_g^{[\star]-1} - b_t^{[\star]} \kappa_0^{[\star]}}{a_z^{[\star]2}} + 2 \frac{b_z^{[\star]} a_t^{[\star]} \kappa_0^{[\star]}}{a_z^{[\star]3}} \right) \left(\frac{k_t}{\kappa_0^{[\star]}} \right)^2 \quad (34)$$

$$C_{EM}^{11(32)} = -n_z \frac{k_t}{a_z^{[\star]}}, \quad C_{EM}^{41[22]} = \frac{a_t^{[\star]}}{a_z^{[\star]}} \frac{k_t}{\kappa_0^{[\star]}}, \quad (35)$$

$$D_{EM}^{11[32]} = -n_z \frac{b_z^{[\star]}}{a_z^{[\star]2}} k_t, \quad D_{EM}^{41[22]} = -[+] \left(\frac{a_t^{[\star]} V_g^{[\star]-1} - b_t^{[\star]} \kappa_0^{[\star]}}{a_z^{[\star]} \kappa_0^{[\star]}} + \frac{b_z^{[\star]} a_t^{[\star]}}{a_z^{[\star]2}} \right) \frac{k_t}{\kappa_0^{[\star]}}, \quad (36)$$

$$C_{ME}^{mn} = -C_{EM}^{nm}, \quad D_{ME}^{mn} = -D_{EM}^{nm} \quad (37)$$

where $n_z = \pm 1$, depending on the sign of Z , that is, $Z \gtrless 0$.

In order to obtain the final form of DDGF for propagating EMFSVAs in the anisotropic medium, we should still get an integral over \vec{k}_t . Unfortunately, this integration cannot be performed analytically in closed form and this integral has to be calculated numerically. Considering source vectors and using Eqs. (15) and (30) together with the following equations, we can numerically investigate the EMFSVAs propagation in any unbound anisotropic dispersive media. The present formalism can be extended, for future work, to contain interface effects, i.e. reflection, and, in turn, applicable to investigate the propagation of EMFSVAs via multilayer media.

For the sake of this section, we examine the formalism for a three-layer non-magnetic uniaxial MM in which an active medium is sandwiched by two impedance-matched passive media, like it was discussed in the introduction. Without any loss of generality, we set $k_y = 0$. Then we consider a Gaussian electric surface current, without any dependence on \hat{y} , as follows

$$J_{my}^E(x', z', t') = J_s e^{-\sigma_x x'^2} e^{-\sigma_t t'^2} \delta(z'), \quad (38)$$

where J_s is a normalization factor. Next, we assume there are equivalent electric and magnetic currents,

$$\vec{J}_{ms}^{E(l)} = \hat{z} \times \vec{H}_{m(l)}, \quad \vec{J}_{ms}^{M(l)} = \vec{E}_{m(l)} \times \hat{z}, \quad (39)$$

on the interface of l^{th} and $(l+1)^{th}$ layers ($l = 1, 2$). Regarding Eqs. (15), (30), (38), and (39), we obtain non-zero electric and magnetic components of EMFSVAs as follows

$$E_{my}^{(1)} = G_{EE}^{22(1)} J_{my}^E, \quad E_{my}^{(l+1)} = G_{EE}^{22(l)} H_{mx}^{(l)} + G_{EE}^{23(l)} E_{my}^{(l)}, \quad (40)$$

$$H_{mx}^{(1)} = G_{EE}^{32(1)} J_{my}^E, \quad H_{mx}^{(l+1)} = G_{EE}^{32(l)} H_{mx}^{(l)} + G_{EE}^{33(l)} E_{my}^{(l)}, \quad (41)$$

$$H_{mz}^{(1)} = G_{ME}^{22(1)} J_{my}^E, \quad H_{mz}^{(l+1)} = G_{ME}^{22(l)} H_{mx}^{(l)} + G_{ME}^{23(l)} E_{my}^{(l)}, \quad (42)$$

where $l = 1, 2$. We assume the second layer is an active non-magnetic, $\mu_{t(z)} = \mu_0$, medium which has the Lorenz dielectric as

$$\varepsilon_L = \varepsilon_0 \left(1 - \frac{\omega_p^2}{\omega_r^2 - \omega_0^2 - i\gamma\omega_0} \right), \quad (43)$$

where $\omega_p/2\pi = 0.42$ GHz, $\omega_r/2\pi = 85.54$ THz, and $\gamma/2\pi = 4$ MHz are the atomic plasma frequency, resonance frequency, and the linewidth of the resonance, respectively [46]. We work far from the resonance frequency and set $\omega_r = 10 \omega_p$, $\gamma = 0.2 \omega_p$, and $\omega_0 = \omega_r + \omega_p/3$ at which the group velocity of envelop is superluminal (cf. Sec. 5). Fig. 1 the propagation of electric and magnetic components of EMFSVAs via the three-layer medium at $t = 0$ (plots in the top) and $t = L/6c$ (s) (plots in the bottom) in which L , the total length of the three-layer slab, is given by $L = 105 l_p$, with $l_p = 2\pi c/\omega_p$ as the plasma wavelength, and c is the light speed in vacuum. We consider the following values of the Gaussian pulse parameters: $\sigma_t = 100(2\pi/\Delta\omega)^2$ with $\Delta\omega = \omega_0/10$, and $\sigma_x = 100\lambda^2$ with $\lambda = 2\pi c/\omega_0$.

After a close looking at superluminal and subluminal group velocities of EMFSVAs in the next section, we shall discuss the simulation results in this context in Sec. 6.

5 Superluminal and Subluminal group velocities

We obtain some frequency intervals in which v_g and v_g^* , the group velocities of EMFSVAs, as given by the formalism for the TM and TE polarizations, respectively, are superluminal or subluminal. Recalling Eq. (28) together with Eqs. (20) and (21) and after some manipulations, we obtain

$$V_g^{[\star]} = \frac{c\sqrt{\zeta_t\zeta_t^* - \zeta_t^{[\star]}/\zeta_z^{[\star]}(k_t/k_0)^2}}{\zeta_t\zeta_t^* (1 + \omega\partial_\omega(\log\sqrt{\zeta_t\zeta_t^*}))_{\omega_0} - \zeta_t^{[\star]}/\zeta_z^{[\star]}(k_t/k_0)^2 \left(\omega\partial_\omega(\log\sqrt{\zeta_t^{[\star]}/\zeta_z^{[\star]}})\right)_{\omega_0}}, \quad (44)$$

for TM [TE] polarization, where $\zeta^{[\star]} = \varepsilon(\mu)$. It should be mentioned that ε and μ , the relative constitutive parameters, and the corresponding derivatives are valued at ω_0 . Setting $k_t = 0$, Eq. (44) is simplified as

$$V_g^{[\star]} = \frac{c}{\partial_\omega(\omega n)_{\omega_0}}, \quad (45)$$

where n , the complex refractive index of the medium, is defined by $n = \sqrt{\varepsilon_t\mu_t}$. For the active medium, Eq. (43), Fig. 2 panel (a) depicts the group velocity, v_g , (solid) and its inverse, the real part of the denominator of Eq. (43), (dashed) in units of $1/c$ for $k_t = 0$ (the black curve), $k_t = \kappa_0/2$ (the red curve), and $k_t = \kappa_0$ (the blue curve). We set $\omega_r = 10$ and $\gamma = 0.2$ in unit of ω_p . The dashed-red curve is compatible to that of Ref. [47]. We shall discuss about the results in Sec. 6.

In order to study the subluminal group velocity of EMFSVAs, we consider a periodic metamaterial formed by thin layers of Si and ITO, where Si stands for silicon and ITO stands for indium-tin oxide, in which ITO is a low-loss plasmonic material. Si has a high constant relative permittivity, $\varepsilon_{\text{Si}} = 11.68$ [26], and the dispersion of permittivity of ITO is described by the Drude model so that the effective relative permittivity of our unbound anisotropic two-layer pattern reads

$$\varepsilon^{eff} = r_1 \left(\varepsilon_\infty - \frac{\omega_p^2}{\omega_0^2 + i\gamma\omega_0} \right) + r_2 \varepsilon_{\text{Si}}, \quad (46)$$

where $\varepsilon_\infty = 4$, $\omega_p = 3.13 \times 10^{15}$ rad/s, $\gamma = 1.07 \times 10^{14}$ s⁻¹ [26], and $r_1 = r_2$. Fig. 2 panel (b) shows the normalized group velocities: at $k_t = 0$, the black curve, at $k_t = \kappa_0^{[\star]}/2$, the red (magenta) curve, and at $k_t = \kappa_0^{[\star]}$, the blue (cyan) curve, for the TM [TE] polarization of EMFSVAs versus ω_0 in terms of eV. We shall come back to discuss about these results in Sec. 6.

6 Discussion and Conclusions

At the end of Sec. 4, we considered a Gaussian pulse which travels through a three-layer slab with a layer in the middle containing a medium with inverted population. The permittivity of the two other layers is the same as the real part of that of the second layer. Thus, the layers are approximately impedance matched and there is no reflections at the interfaces of layers. According to top plots in Fig. 1, at $t = 0$, the tail of our primary Gaussian pulse penetrates into the second layer (the active layer). We can see that there are two propagating pulses in the second layer: one propagates backward and the second one, which is amplified, continues to go forward and penetrates into the third layer. The penetrated amplified pulse continues the propagation via the third layer, which is a lossless medium. As time goes by, the original envelop passes through the first layer so that after $t = L/6c$ s its peak arrives at the middle of the layer. Similarly, at the second layer, both backward and forward propagating pulses become weak while at the third layer the amplified precursor pulse is at the middle of the medium without any attenuation. It should be noted that the pulse exits the second layer before it would have traveled through an equal distance of vacuum. This is because of lacking a definite edge of the Gaussian pulse.

Regarding Fig. 2 panel (a), as we can see, when $\omega_0/\omega_p \lesssim 9.48$ and $\omega_0/\omega_p \gtrsim 10.48$ for the case of $k_t = 0$ there is superluminality with a maximum value of $V_g \simeq 2c$ whereas in the case of $k_t \neq 0$ we have superluminal phenomenon just for $9.08 \lesssim \omega_0/\omega_p \lesssim 9.46$ and $10.52 \lesssim \omega_0/\omega_p \lesssim 10.88$ intervals with a maximum value of $V_g \simeq 1.5c$. Moreover, when $\omega_0/\omega_p \simeq 9.5, 9.8, 10.1, 10.5$, EMFSVAs are stopped (ultra-subluminality). There are also two frequency intervals within which the group velocity is negative. As k_t increases, we can see the magnitude of the V_g decreases as we expect from Eq. (44).

Fig. 2 panel (b) depicts the subluminality of the envelop passing via a periodic layered slab of Si - ITO. For the $k_t \neq 0$, there is a difference between V_g and V_g^* because of the different values of the coefficients of k_t in Eq. (44) for the TM and the TE polarizations, respectively. By increasing k_t , the group velocity of the envelop with TM polarization gets reduced as compared with the TE case. Indeed, when k_t increases, the second term of the denominator of V_g becomes greater than the first term, whereas in the case of V_g^* , the relevant term gets zero. Hence, for the TM polarization case the order of plots can change for some values of k_t . On the other hand, in the case of TM polarization the magnitude of the group velocity of the envelop approaches zero faster than in the TE polarization case, with respect to the same decreasing rate of ω_0 .

Now, let us consider if it was reasonable to ignore the $O(\Omega^2)$ terms in Eq. (26). In order to answer this question, we define the smallness parameter: the ratio of the third term to the second one in Eq. (26), as follows

$$\delta_g^{[\star]} = \frac{\Delta\omega}{2\kappa_0^{[\star]}} \left\{ -\frac{1}{V_g^{[\star]}} + V_g^{[\star]} \left[b_t b_t^{[\star]} + \frac{b_z^{[\star]}}{a_z^{[\star]3}} \left(b_t^{[\star]} a_z^{[\star]} - b_z^{[\star]} a_t^{[\star]} \right) k_t^2 \right] \right\} \quad (47)$$

where we replace Ω with its maximum value, i.e $\Delta\omega$. Obviously, $\delta_g^{[\star]}$ depends on ω_0 and $\Delta\omega$ beside of the material properties. Now, we emphasize that the reliability of the superluminality and ultra-slowness of EMFSVAs depends on the magnitude of δ_g . For the active and passive media considered above, $\delta_g^{max} \sim 0.25$, except in the case of $v_g^{TM}(k_t = \kappa_0)$ for which $\delta_g^{max} \sim 0.7 - 0.75$ in all over ω_0 .

To conclude, the considered examples confirm the applicability and validity of the DDGF approach developed in this work. The observed phenomena in the three-layer structure with an active layer are qualitatively similar to the ones that were previously reported in literature [47]. The group velocity obtained in our formalism agrees with the standard definition and results in similar behaviors in the superluminal and subluminal cases considered in this article and the literature.

Acknowledgement

The authors acknowledge financial support under the project Ref. UID/EEA/50008/2013, sub-project SPT, financed by Fundação para a Ciência e a Tecnologia (FCT)/Ministério da Ciência, Tecnologia e Ensino Superior (MCTES), Portugal.

References

- [1] H. Lamb, *Hydrodynamics* (Cambridge, University Press, 1916).
- [2] A. Schuster, *An introduction to the theory of optics* (London, Edward Arnold, 1904).
- [3] L.I. Mandelshtam, Zh. Eksp. Teor. Fiz. **15**, 475 (1945).
- [4] V.G. Veselago, Sov. Phys. Uspekhi. **10**, 509 (1968).
- [5] L. J. Wang, A. Kuzmich, and A. Dogariu, Nature **406**, 277 (2000).
- [6] D. R. Smith, J. B. Pendry, and M. C. K. Wiltshire, Science **305**, 788 (2004).
- [7] U. Leonhardt, Nature **415**, 406 (2002).
- [8] J. B. Pendry, D. Schurig, and D. R. Smith, Science **312**, 1780 (2006).
- [9] N.I. Landy, S. Sajuyigbe, J.J. Mock, D.R. Smith, and W.J. Padilla, Phys. Rev. Lett. **100**, 207402 (2008).
- [10] J. Zhang, K. F. MacDonald, and N. I. Zheludev, Light: Sci. Appl. **1**, 18 (2012).
- [11] Z. Liu, H. Lee, Y. Xiong, C. Sun, and X. Zhang, Science **315**, 1686 (2007).
- [12] D. Schurig, J. J. Mock, B. J. Justice, S. A. Cummer, J. B. Pendry, A. F. Starr, and D. R. Smith, Sci. **314**, 977 (2001).
- [13] H.-T. Chen, W. J. Padilla, J. M. O. Zide, A. C. Gossard, A. J. Taylor, and R. D. Averitt, Nature **444**, 597 (2006).
- [14] T. Driscoll, H.-T. Kim, B.-G. Chae, B.-J. Kim, Y.-W. Lee, N. M. Jokerst, S. Palit, D. R. Smith, M. Di Ventra, and D. N. Basov, Science **325**, 1518 (2009).
- [15] N.-H. Shen, M. Massaouti, M. Gokkavas, J.-M. Manceau, E. Ozbay, M. Kafesaki, T. Koschny, S. Tzortzakis, and C. M. Soukoulis, Phys. Rev. Lett. **106**, 037403 (2011).
- [16] M.G. Silveirinha and S.I. Maslovski, Phys. Rev. Lett. **105**, 189301 (2010).
- [17] A. Boltasseva and H.A. Atwater, Science **331**, 290 (2011).
- [18] I.V. Shadrivov, P.V. Kapitanova, S.I. Maslovski, and Y.S. Kivshar, Phys. Rev. Lett. **109**, 083902 (2012).
- [19] T.A. Morgado, J.S. Marcos, S.I. Maslovski, and M.G. Silveirinha, Appl. Phys. Lett. **101**, 021104 (2012).
- [20] K. Joulain, J. P. Mulet, F. Marquier, R. Carminati, and J. J. Greffet, Surf. Sci. Rep. **57**, 59 (2005).
- [21] S.I. Maslovski, C.R. Simovski, S.A. Tretyakov, New J. Phys. **18**, 013034 (2016).

[22] I. Latella, S.-A. Biehs, R. Messina, A.W. Rodriguez, and P. Ben-Abdallah, Phys. Rev. B **97** 035423 (2018).

[23] C. Simovski, S. Maslovski, I. Nefedov, and S. Tretyakov, Opt. Express 21, 12, 14988 (2013).

[24] T. Inoue, K. Watanabe, T. Asano, and S. Noda, Opt. Express 26, 2, 192 (2018).

[25] S. Chu and S. Wong, Phys. Rev. Lett. **48**, 11, 738 (1982).

[26] K.L. Tsakmakidis, T.W. Pickering, J.M. Hamm, A.F. Page, and O. Hess, Phys. Rev. Lett. **112**, 167401 (2014).

[27] M.S. Bigelow, N.N. Lepeshkin, R.W. Boyd, Science **301** 200 (2003).

[28] A.D. Neira, G.A. Wurtz, and A.V. Zayats, Nature **5**, 17678 (2015).

[29] P.M. Valanju, R.M. Walser, and A.P. Valanju, Phys. Rev. Lett. **88**, 187401 (2002).

[30] S.I. Maslovski, URSI IEEE XXVII national convention on radio science, Espoo, Innopoli (2002).

[31] M.I. Stockman, Phys. Rev. Lett. **98**, 177404 (2007).

[32] D. Forcella, C. Prada, R. Carminati, Phys. Rev. Lett. **118**, 134301 (2017).

[33] M. M. Kash, V. A. Sautenkov, A. S. Zibrov, L. Hollberg, G. R. Welch, M. D. Lukin, Y. Rostovtsev, E. S. Fry, and M. O. Scully, Phys. Rev. Lett. **82**, 26, 5229 (1999).

[34] L. M. Duan, M. D. Lukin, J. I. Cirac, and P. Zoller, Nature **414**, 6862, 413 (2001).

[35] M. D. Lukin and A. Imamoğlu, Nature **413**, 6853, 273 (2001):

[36] C. Liu, Z. Dutton, C. H. Behroozi, and L. V. Hau, Nature **409**, 6819, 490 (2001).

[37] D. F. Phillips, A. Fleischhauer, A. Mair, R. L. Walsworth, and M. D. Lukin, Phys. Rev. Lett. **86**, 783 (2001).

[38] M.S. Shahriar, G. S. Pati, R. Tripathi, V. Gopal, M. Messall, and K. Salit, Phys. Rev. A **75**, 5, 053807 (2007).

[39] M. Bajcsy, S. Hofferberth, V. Balic, T. Peyronel, M. Hafezi, A. S. Zibrov, V. Vuletic, and M. D. Lukin, Phys. Rev. Lett. **102**, 20, 203902 (2009).

[40] M. Lee, M.E. Gehm, and M.A. Neifeld, J. Opt. **12**, 10 (2010).

[41] S. Hrabar, I. Krois, I. Bonic, and A. Kiricenko, Appl. Phys. Lett. **102**, 054108 (2013).

[42] M. Khorasaninejad, W.T. Chen, J. Oh, and F. Capasso, Nano Lett. **16**, 3732 (2016).

[43] H. N. S. Krishnamoorthy, Z. Jacob, E. Narimanov, I. Kretzschmar, and V. M. Menon, Science **336**, 205 (2012).

[44] G. A. Wurtz, et al. Nat. Nanotech. **6**, 107 (2011).

[45] A. Poddubny, I. Iorsh, P. Belov, and Y. Kivshar, Nat. Phot. **7**, 948 (2013).

[46] I.V. Lindell, IEE Proc-Sci. Meas. Technol. **143**, 2 (1996).

[47] E.L. Bolda, J.C. Garrison, and R.Y. Chiao, Phys. Rev. A 49 4 (1994).

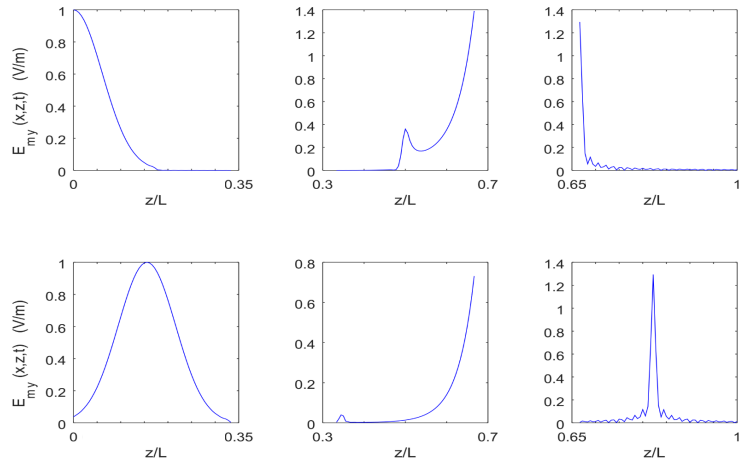


Figure 1: The propagation of electric and magnetic components of EMFSVAs, at $t = 0$ (top plots) and $t = L/6c$ (s) (bottom plots), via a three-layer medium in which the second layer has the Lorentzian dielectric with gain and the permittivities of the first and third layers are the same as the real part of the permittivity of the second one (see text).

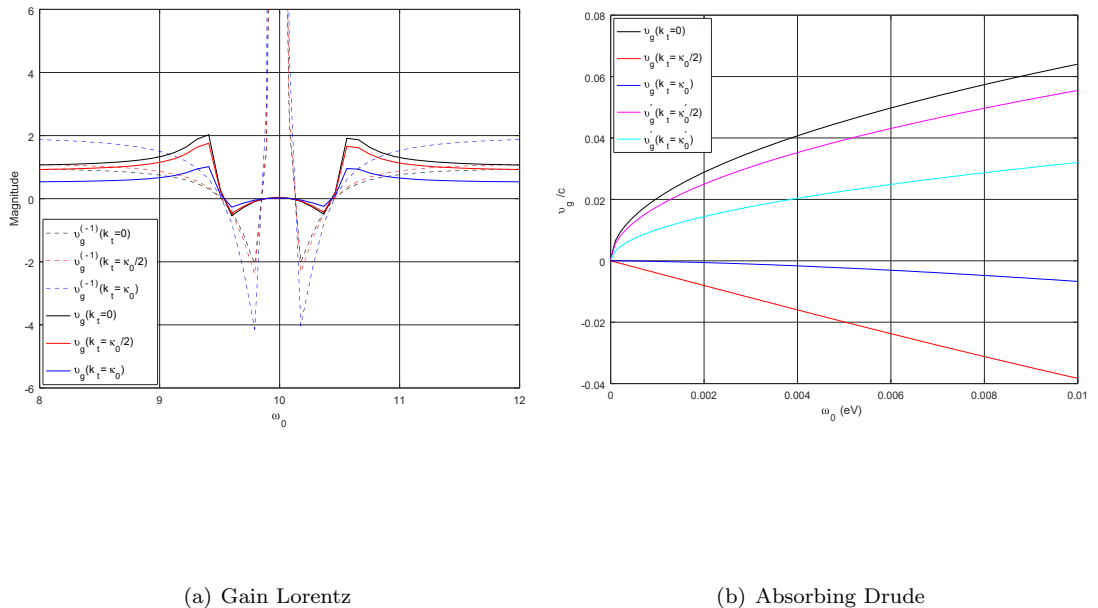


Figure 2: (a) The normalized group velocities (solid) and the corresponding reciprocal ones (dashed) of propagating EMFSVAs in a Lorentzian dielectric with gain for $k_t = 0$ (black curves), $\kappa_0/2$ (red curves), κ_0 (blue curves). (b) The normalized group velocities of propagating EMFSVAs via a two-layer Drude dielectric (Si-ITO): at $k_t = 0$, the black curve, at $k_t = \kappa_0^{[*]}/2$, red (magenta), and at $k_t = \kappa_0^{[*]}$, the blue (cyan) curve, for the TM [TE] polarization, vs. ω_0 in terms of eV .